nature neuroscience

Cyclin-dependent kinase 5 governs learning and synaptic plasticity via control of NMDAR degradation

Ammar H Hawasli[1,5], David R Benavides[1,5], Chan Nguyen[1], Janice W Kansy[1], Kanehiro Hayashi[1], Pierre Chambon[2], Paul Greengard[3], Craig M Powell[1,4], Donald C Cooper[1] & James A Bibb[1]

Learning is accompanied by modulation of postsynaptic signal transduction pathways in neurons. Although the neuronal protein kinase cyclin-dependent kinase 5 (Cdk5) has been implicated in cognitive disorders, its role in learning has been obscured by the perinatal lethality of constitutive knockout mice. Here we report that conditional knockout of Cdk5 in the adult mouse brain improved performance in spatial learning tasks and enhanced hippocampal long-term potentiation and NMDA receptor (NMDAR)-mediated excitatory postsynaptic currents. Enhanced synaptic plasticity in Cdk5 knockout mice was attributed to reduced NR2B degradation, which caused elevations in total, surface and synaptic NR2B subunit levels and current through NR2B-containing NMDARs. Cdk5 facilitated the degradation of NR2B by directly interacting with both it and its protease, calpain. These findings reveal a previously unknown mechanism by which Cdk5 facilitates calpain-mediated proteolysis of NR2B and may control synaptic plasticity and learning.

The cellular and molecular mechanisms underlying declarative learning and memory constitute a predominant area in basic neurobiological research and are of considerable clinical relevance. A generally accepted hypothesis is that memories are formed in specific circuits of the brain through changes in the strength of neuronal synapses[1]. One form of synaptic plasticity, long-term potentiation (LTP), seems to be a critical component of information processing and memory storage in the hippocampus[1,2]. Information storage at the behavioral and cellular levels depends on neurotransmitter receptor complexes and downstream intracellular signaling cascades. Obtaining a better understanding of these biochemical pathways is a crucial step in delineating the processes controlling learning and synaptic plasticity.

The proline-directed serine/threonine protein kinase Cdk5, together with its neuronal-specific activating cofactors p35 and p39, have been implicated in a plethora of normal and pathological processes in the mammalian CNS[3–12]. However, assessment of Cdk5's function in learning and synaptic plasticity has been limited by congenital abnormalities in constitutive knockout mice[9] and by pharmacological nonspecificity[13].

To circumvent these confounds, we examined the effects of conditional Cdk5 knockout on contextual and spatial learning and synaptic plasticity. Loss of Cdk5 in the adult brain improved performance in hippocampal behavioral learning tasks, enhanced synaptic plasticity and elevated currents through NMDARs. Biochemical and neurophysiological analyses showed that the enhanced plasticity in Cdk5 knockout mice was due to changes in NR2B subunit degradation. These findings reveal a previously unknown pathway through which Cdk5 may regulate ionotropic glutamate receptor constituency via protein-protein interactions.

RESULTS

Conditional loss of Cdk5 in the adult mouse brain

We generated an inducible conditional Cdk5 knockdown model to study the role of Cdk5 in learning and synaptic plasticity. This Cre/*loxP* system allowed temporal control of Cdk5 gene deletion in the adult brain. Using homologous recombination, exons encoding vital Cdk5 catalytic-domain components were flanked with *loxP* elements (floxed; **Fig. 1a**). Homozygous floxed Cdk5 mice were crossed with animals bearing an inducible Cre-ER^T recombinase transgene under the control of the prion protein promoter[14].

Conditional Cdk5 knockdown in homozygous floxed mice carrying the Cre transgene was achieved by administration of hydroxytamoxifen, an estrogen receptor antagonist that induces nuclear translocation of the Cre-ER^T recombinase[14]. Hydroxytamoxifen-dosed homozygous floxed mice lacking the Cre-ER^T transgene showed no loss of Cdk5 and served as controls (wild type; **Supplementary Fig. 1** online). Floxed alleles, transgenic alleles and drug treatment had no effects on Cdk5 levels. Furthermore, Cdk5 knockout did not alter basic hippocampal cytoarchitecture (**Supplementary Fig. 1**). Empirically optimized drug treatment reduced Cdk5 mRNA levels in whole hippocampus, striatum, cortex, cerebellum, hippocampal CA1 and CA3, and dentate gyrus layers by 45.7 ± 8.8%, 59.3 ± 8.3%, 75.9 ± 7.4%, 73.8 ± 6.8%, 71.4 ± 3.0%, 55.7 ± 3.2% and 49.0 ± 2.6%, respectively, compared with wild type (**Fig. 1b** and **Supplementary Fig. 1**). Real-time polymerase

[1]Department of Psychiatry, University of Texas Southwestern Medical Center, 5323 Harry Hines Blvd., Dallas, Texas 75390, USA. [2]Institut de Génétique et de Biologie Moléculaire et Cellulaire, 67404 Illkirch Cedex, Centre Universitaire de Strasbourg, France. [3]Laboratory of Molecular and Cellular Neuroscience, The Rockefeller University, 1230 York Avenue, New York, New York 10021, USA. [4]Department of Neurology, University of Texas Southwestern Medical Center, 5323 Harry Hines Blvd., Dallas, Texas 75390, USA. [5]These authors contributed equally to this work. Correspondence should be addressed to J.A.B. (james.bibb@utsouthwestern.edu).

Received 20 February; accepted 3 May; published online 27 May 2007; doi:10.1038/nn1914

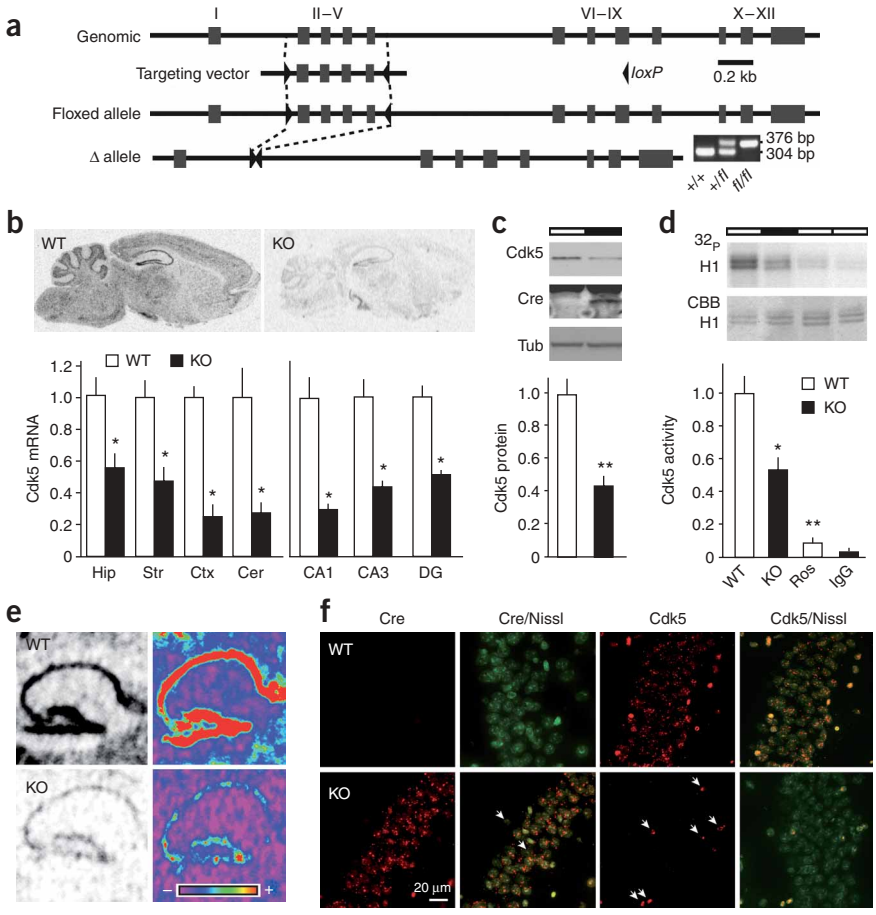

Figure 1 Conditional loss of Cdk5 in adult mouse hippocampus. (**a**) Cdk5 gene targeting strategy. Inset, PCR genotyping of wild-type (+) and floxed (*fl*) alleles. (**b**) Radiolabeled *in situ* with quantification for hippocampus (Hip), striatum (Str), cortex (Ctx), cerebellum (Cer) and hippocampal layers ($n = 6$–8) of wild-type (WT) and knockout (KO) mice. (**c**) Quantitative immunoblots of Cdk5, Cre and α-tubulin (Tub) in hippocampal homogenates ($n = 20$). (**d**) Cdk5 kinase activity immunoprecipitated from hippocampus. Radiolabeled (^{32}P-H1) and Coomassie-stained (CBB) H1 histone from WT and KO mice were compared with roscovitine (Ros) and IgG controls ($n = 6$). (**e**) Radiolabeled *in situ* for hippocampal Cdk5 mRNA with pseudocolor quantification (+ = high, − = low) (**f**) Cdk5 and Cre mRNA fluorescent *in situ* hybridizations with Nissl counterstains in WT and KO CA1 pyramidal neurons. Arrows show neurons with no Cre mRNA or no Cdk5 loss. Data represent mean ± s.e.m.; $^{*}P < 0.05$, $^{**}P < 0.01$, versus WT; Student's *t*-test.

chain reaction (RT-PCR) revealed a 43.6 ± 6.8% reduction in whole hippocampus Cdk5 mRNA (**Supplementary Fig. 1**). Decreases in hippocampal Cdk5 protein level (59.2 ± 4.9%, **Fig. 1c**) and activity (44.1 ± 0.2%, **Fig. 1d**) were detected by quantitative immunoblots and immunoprecipitation kinase assays, respectively. Pseudocolor quantification of Cdk5 mRNA also showed a robust knockdown of Cdk5 message in hippocampal layers (**Fig. 1e**). High-resolution confocal analyses of fluorescent *in situ* hybridizations (FISH) were conducted to assess Cdk5 knockout in CA1 neurons. FISH showed that 90.9 ± 7.7% of cells in the stratum pyramidale of Cdk5 knockout lacked Cdk5 mRNA (**Fig. 1f**). An equivalent proportion of CA1 cells in Cdk5 knockout mice expressed the Cre-ER^{T} mRNA (**Fig. 1f**). Thus, temporally controlled, conditional loss of Cdk5 was achieved, allowing for the study of hippocampus-dependent learning and synaptic plasticity.

Improved performance in hippocampal learning tasks

The role of Cdk5 in associative learning and memory was evaluated via contextual and cued fear-conditioning behavioral tests. Animals were placed in a novel context, analyzed for baseline behavior, and exposed to cue/foot shock pairings. Memory to context was assessed by examining freezing behavior 24 h after training. Cdk5 knockout mice showed significantly increased contextual memory (61.4 ± 4.1% for knockout versus 42.1 ± 3.8% for wild type; **Fig. 2a**). No significant differences were observed in baseline freezing, cue-conditioned memory, nociception, locomotion, anxiety or preknockout memory (**Fig. 2a**, **Supplementary Fig. 2** online). The increased freezing upon re-exposure to context indicates enhanced hippocampus-dependent memory.

We examined the rate and extent of contextual fear-extinction by re-exposing the animals to the conditioned context over several trials. Cdk5 knockout mice showed greater contextual extinction, as evidenced by significantly less freezing during the fourth re-exposure, 96 h after training (29.8 ± 4.4% for knockout versus 71.1 ± 12.6% for wild type, **Fig. 2b**; **Supplementary Fig. 2**). Thus, conditional Cdk5 knockout resulted in increased hippocampus- and NMDAR-dependent[15] cognitive flexibility.

To assess the effect of conditional Cdk5 knockout on spatial learning and memory, we used the hippocampus- and NMDAR-dependent water-maze task[16,17]. Animals were trained to find a submerged platform using distant visual cues, after which the platform was removed to test spatial memory. We then assessed hippocampus-dependent[17–19] cognitive flexibility by retraining the mice to find a platform in the opposite quadrant (reversal). Although both genotypes showed equally successful learning during initial training sessions (**Fig. 2c**), knockout mice showed shortened escape latencies during the reversal task (**Fig. 2d**). The enhancement of reversal learning was apparent as early as the second trial of day 1 and first trial of day 2, indicating single-trial and long-term spatial learning enhancements (**Fig. 2d**). Reversal differences were not due to disparities in velocity (**Supplementary Fig. 2**). Better reversal learning was accompanied by superior spatial memory, as assessed by a platform-removal probe trial. Although both genotypes showed significant preferences for the target quadrant after 11 d of training (**Fig. 2c**), only knockout mice showed a preference for the new target region after reversal training (**Fig. 2d**). Therefore, conditional Cdk5 knockout resulted in improved performance in the hippocampus-dependent[17] reversal spatial learning task.

Enhanced synaptic plasticity and NMDAR-mediated currents

Because alterations in the strength of synaptic connection between hippocampal neurons are believed to underlie contextual and spatial memories[1,16], we analyzed synaptic plasticity in the hippocampal Schaffer collateral pathway (SC-CA1). No differences between wild-type and knockout groups were observed in AMPA receptor–mediated synaptic transmission or paired-pulse facilitation (PPF; **Fig. 3a**), as

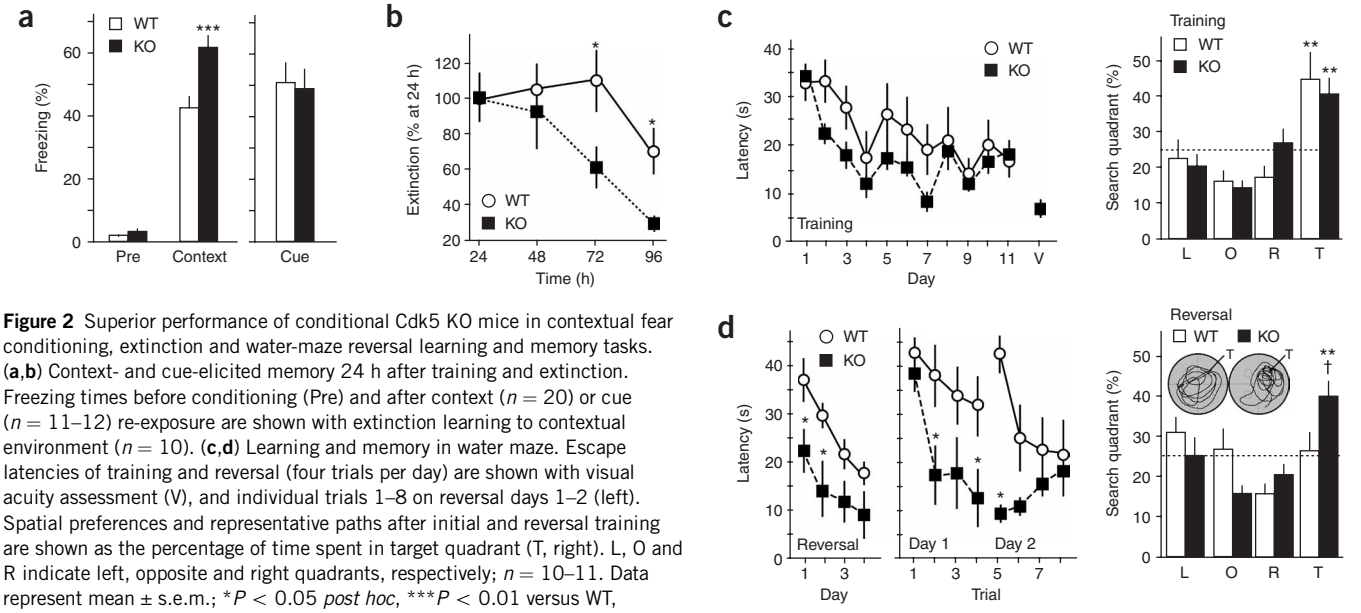

Figure 2 Superior performance of conditional Cdk5 KO mice in contextual fear conditioning, extinction and water-maze reversal learning and memory tasks. (**a**,**b**) Context- and cue-elicited memory 24 h after training and extinction. Freezing times before conditioning (Pre) and after context ($n = 20$) or cue ($n = 11$–12) re-exposure are shown with extinction learning to contextual environment ($n = 10$). (**c**,**d**) Learning and memory in water maze. Escape latencies of training and reversal (four trials per day) are shown with visual acuity assessment (V), and individual trials 1–8 on reversal days 1–2 (left). Spatial preferences and representative paths after initial and reversal training are shown as the percentage of time spent in target quadrant (T, right). L, O and R indicate left, opposite and right quadrants, respectively; $n = 10$–11. Data represent mean ± s.e.m.; $^{*}P < 0.05$ *post hoc*, $^{***}P < 0.01$ versus WT, $^{**}P < 0.05$ versus other quadrants, $^{\dagger}P < 0.05$ versus WT in T; Student's *t*-test.

measured by extracellularly recorded field excitatory postsynaptic potentials (fEPSPs). A weak theta-burst stimulus (2× TBS) had no effect on wild type (2.0 ± 6.9% change from baseline), but induced robust LTP in knockout slices (34.0 ± 4.0%; **Fig. 3b**,**c**). We obtained similar results after a weak 50-Hz tetanus (0.1 ± 2.3% for wild type versus 31.1 ± 5.9% for knockout; **Fig. 3c**). A stronger theta-burst stimulation (3× TBS) induced LTP of similar magnitude in wild-type and knockout slices (34.2 ± 6.3% versus 49.7 ± 1.0%, respectively; **Fig. 3b**,**c**), and elevated post-tetanic potentiation in knockout slices relative to wild type (123.4 ± 8.9% versus 52.4 ± 14.7%, respectively; **Fig. 3b**). Strong 100-Hz tetanus also produced equivalent LTP in wild-type and knockout slices (48.3 ± 5.4% versus 49.1 ± 4.9%, respectively; **Fig. 3c**). These results indicated that Cdk5 knockout reduced the induction threshold for LTP in the SC-CA1 pathway.

To investigate the LTP enhancement mechanism, we assessed the relative contribution of synaptically evoked NMDAR-mediated current. The relationship of stimulus intensity to fiber-volley magnitude was equivalent between groups, indicating a lack of differential axonal stimulation (data not shown). In addition, there were no disparities in AMPA receptor–mediated synaptic transmission (**Fig. 3a**) or whole-cell currents (3,601 ± 400 versus 3,800 ± 313 charge for wild type and knockout; $P = 0.71$, Student's *t*-test). Voltage measurements in field recordings from Cdk5 knockout slices revealed increased NMDAR-mediated synaptic transmission and a 9.0 ± 2.4-fold larger NMDA/AMPA fEPSP ratio versus wild type (**Fig. 3d**). Whole-cell voltage-clamp synaptically evoked NMDAR-mediated excitatory postsynaptic currents ($EPSC_{NMDA}$) in CA1 pyramidal neurons revealed no difference in NMDAR reversal potential, but did show a 1.4 ± 0.2-fold larger NMDA/AMPA EPSC ratio (**Fig. 3e** and **Supplementary Fig. 3** online). Thus, loss of Cdk5 resulted in larger NMDAR-mediated fEPSPs and currents.

Increases in NR2B account for enhanced plasticity

NMDAR-mediated current in the adult hippocampal SC-CA1 pathway is predominantly mediated by receptor complexes consisting of NR1 and NR2A and/or NR2B subunits[20]. We determined the relative subunit contributions to the increased $EPSC_{NMDA}$ by measuring sensitivity to an NR2B-selective inhibitor, ifenprodil[21,22]. Ifenprodil-sensitive $EPSC_{NMDA}$ charges were 3.2 ± 0.5-fold greater in Cdk5 knockout slices compared with wild type (**Fig. 4a**). Consistent with this observation, the decay constant for the $EPSC_{NMDA}$ was longer in knockout (74.2 ± 7.2 ms) than wild type (51.5 ± 4.7 ms, **Fig. 4a**). Notably, immunoblot analysis of Cdk5 knockout hippocampal homogenates revealed a 1.33 ± 0.07-fold increase in NR2B levels, whereas NR2A, NR1, and GluR1 levels were unaltered (0.86 ± 0.06, 0.96 ± 0.11, and 0.99 ± 0.18 versus wild type, respectively; **Fig. 4b**). Furthermore, cell-surface receptor–labeling experiments showed a 1.9 ± 0.2-fold increase in NR2B surface-to-total ratio in knockout slices (**Fig. 4c**). This correlated with a hippocampus-specific 2.0-fold increase in synaptosomal NR2B (**Supplementary Fig. 4** online), indicating that the increase in surface NR2B was manifested at synapses. These findings suggest that Cdk5 knockout altered NMDAR constituency owing to increased synaptic and surface levels of NR2B. Consequently, total and ifenprodil-sensitive NMDAR-mediated currents were both elevated.

We also evaluated the contribution of increased NR2B-containing NMDAR-mediated current to the enhancement of plasticity in conditional Cdk5 knockout mice. As previously reported[23], the NR2B-selective inhibitor ifenprodil had no effect on LTP induction in wild-type slices after a sufficient tetanus (48.8 ± 3.5% change from baseline, $n = 3$), confirming that NR2B-containing receptors are not obligatory for SC-CA1 LTP induction in normal adult mice. The LTP enhancement in Cdk5 knockout mice was reversed by ifenprodil (2.3 ± 3.5%) or a general NMDAR antagonist (AP5, 0.5 ± 0.9%; **Fig. 4d**). Therefore, the increase in synaptic plasticity resulting from Cdk5 knockout may be attributed to increased current through NR2B-containing receptors.

Cdk5 knockout reduced calpain-mediated NR2B degradation

The increase in the amount of NR2B could be due to increased gene expression or reduced protein degradation. Analysis of Cdk5 knockout hippocampal tissue by RT-PCR showed no increase in NR2B mRNA (**Supplementary Fig. 4**), suggesting a post-transcriptional mechanism. NMDA is known to induce degradation of NR2B by calpain, a Ca^{2+}-dependent protease[24–26]. We detected significantly less

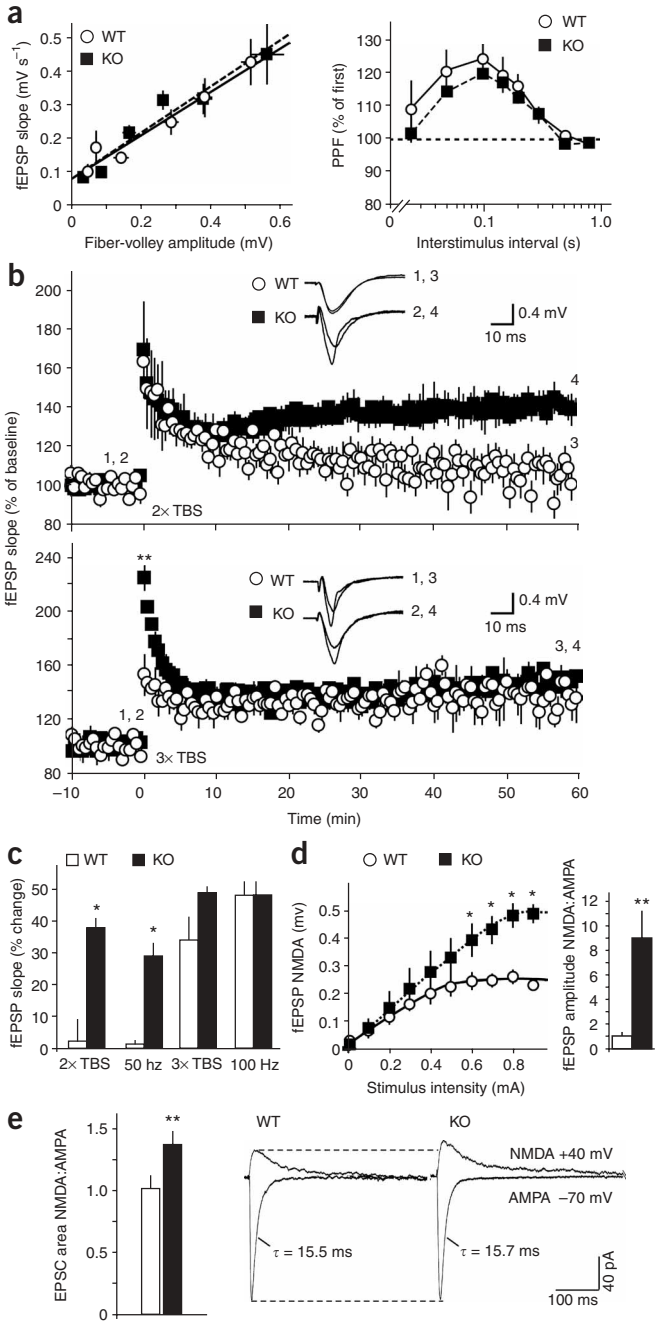

Figure 3 Enhanced synaptic plasticity and NMDAR-mediated currents in the hippocampal SC-CA1 pathway of conditional Cdk5 KO mice. (**a**) Basal input/output curve and PPF (50–800-ms interstimulus interval); $n = 7$–9 slices, 5 animals per genotype. (**b**) LTP after 2× TBS and 3× TBS plotted as percent of baseline (–10 to 0 min). Representative traces at baseline (1,2) and 60 min (3,4) are shown. (**c**) LTP 57–60 min after 2× TBS, 50 Hz, 3× TBS and 100 Hz represented as percent change from baseline ($n = 7$–8 slices, 4–5 animals per group). (**d**) NMDAR-mediated fEPSP (fEPSP NMDA) input/output relationship and NMDA/AMPA ratio. AMPA- and NMDA-mediated fEPSPs were measured in 2 and 0 mM Mg^{2+} and 0 and 20 μM DNQX, respectively ($n = 6$ slices, 3 animals per genotype). (**e**) Whole-cell NMDA/AMPA EPSC charge ratio with representative traces. AMPA- and NMDA-mediated EPSCs were measured at –70 mV and +40 mV/20 μM DNQX, respectively ($n = 7$–10 cells, 5–7 animals per genotype). The τ is shown for AMPA-mediated EPSCs. Data represent mean ± s.e.m.; $^*P < 0.05$ *post hoc*, $^{**}P < 0.05$ versus WT; Student's *t*-test.

calpain-mediated NR2B degradation after NMDAR activation in hippocampal knockout slices than in controls (3.6 ± 12.8% and 22.5 ± 8.2% of wild type after 30 and 60 min, respectively; **Fig. 4e**). Furthermore, Cdk5/p25 markedly enhanced calpain-mediated cleavage of the NR2B C terminus *in vitro* (**Fig. 4f**). These *ex vivo* and *in vitro* findings indicate that Cdk5 normally facilitates calpain-mediated cleavage of NR2B.

Cdk5 could affect calpain-mediated cleavage of NR2B via either phosphorylation or direct binding. However, Cdk5 phosphorylated neither calpain (data not shown) nor NR2B *in vitro* (**Supplementary Fig. 4**), and it activated calpain in the absence of Mg^{2+} and ATP (**Fig. 4f**). Thus, cleavage enhancement was independent of kinase activity. On the other hand, NR2B, Cdk5, p35 and calpain coimmunoprecipitated with one another and the postsynaptic density marker PSD-95 in wild-type hippocampal lysates (**Fig. 4g**). Furthermore, Cdk5 knockout reduced the coimmunoprecipitation of NR2B with Cdk5 to 23.1 ± 2.6% that in wild-type controls (**Supplementary Fig. 5** online). Although equal amounts of the Cdk5 cofactor p35 immunoprecipitated from wild-type and knockout lysates, the amount of NR2B associated with p35 was reduced to 48.4 ± 4.8% compared with wild type (**Supplementary Fig. 5**). These data indicate that NR2B, Cdk5, p35 and calpain are in a postsynaptic complex and Cdk5 mediates the interactions between NR2B and p35. NR2B–PSD-95 interaction ratios were unaffected by Cdk5 knockout (**Supplementary Fig. 5**). Finally, *in vitro* pull-down assays demonstrated that resin-conjugated NR2B bound Cdk5 and calpain, and resin-conjugated Cdk5 bound NR2B and calpain (**Fig. 4h**). These findings suggest that Cdk5 binds calpain and NR2B, thereby facilitating cleavage of NR2B. Thus, elevated NR2B levels in the Cdk5 knockout hippocampus likely resulted from the loss of these critical protein-protein interactions.

DISCUSSION

The effects of conditional Cdk5 knockout reveal a previously unknown role for Cdk5 in regulating glutamate receptor degradation. Previous reports separately implicate both Cdk5 (refs. 5–7,9) and CA1 hippocampal NMDARs[1,15,16,20,22,23,27–29] in spatial learning and synaptic plasticity. The present study demonstrates that conditional loss of Cdk5 caused an increase in the amount of NR2B-containing NMDARs and related currents. Notably, transgenic overexpression of the NR2B subunit[15] resulted in learning and plasticity enhancements that were similar to those of Cdk5 knockout mice. Our data also show that NR2B degradation was facilitated by interactions between Cdk5, calpain and NR2B. These findings are consistent with previous reports showing that calpain is a major component of the NMDAR complex[30] and that calpain-mediated cleavage of NR2B decreases the number of functional NMDARs[25,26]. Cdk5 may function structurally to increase interactions between NR2B and calpain and to facilitate NR2B degradation in response to synaptic activity. Calpain also cleaves Cdk5's activating cofactors[31] and numerous Cdk5 substrates[32]. In addition, PSD-95 has been suggested to regulate NMDAR degradation by calpain[33]. Cdk5 has also been reported to modulate PSD-95 levels[34] and may thus contribute to the modulation of NMDARs via multiple pathways.

Ultimately, the increase in NR2B-containing NMDARs may lengthen the integration time window for NMDAR coincidence detection[15] and decrease the threshold to induce the long-term synaptic changes. Consistent with previous reports[35,36], the increase in NMDAR-mediated current and reduction in plasticity threshold may facilitate information processing and learning. Although these findings advance our understanding of Cdk5's role in learning and plasticity, it is important to note that to further understand the molecular mechanism

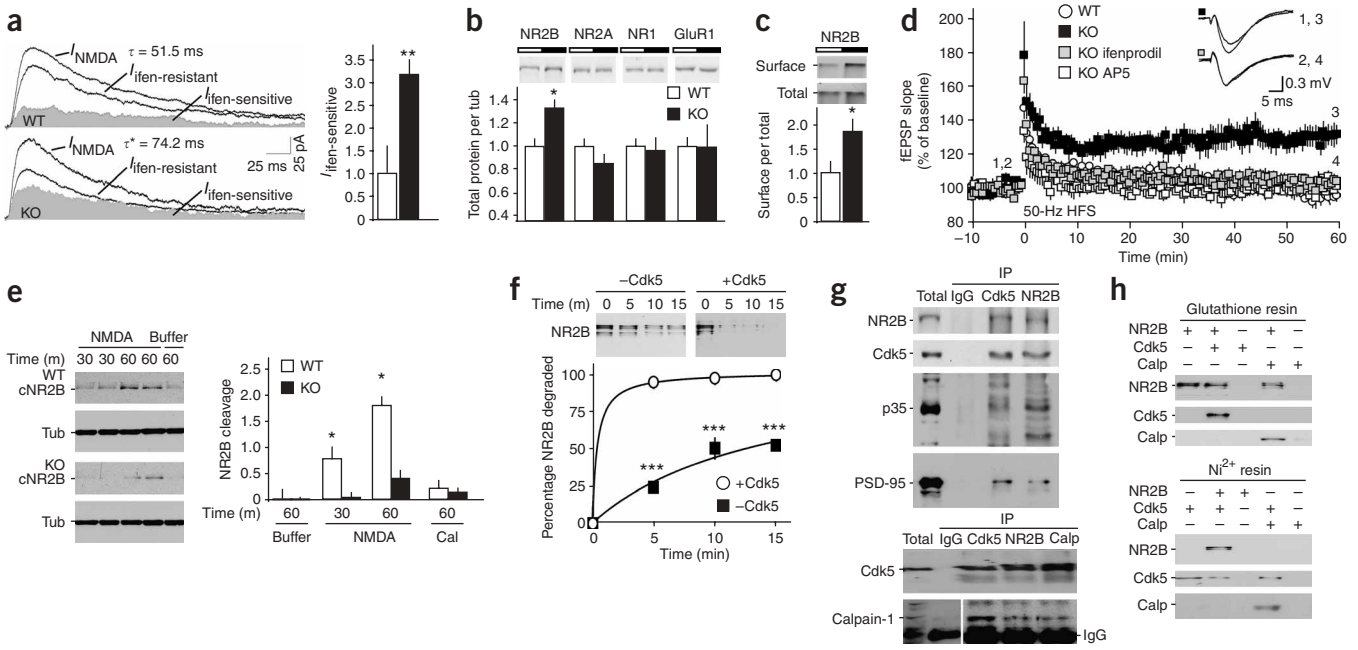

Figure 4 Increased ifenprodil-sensitive NMDAR-mediated current and NR2B levels as a result of reduced calpain activity account for enhanced synaptic plasticity in Cdk5 KO mice. (**a**) Effect of ifenprodil (ifen) on NMDAR-mediated EPSCs. Representative traces of NMDAR-mediated EPSCs before (I_{NMDA}) and after ($I_{ifen\text{-}resistant}$) treatment with 10 μM ifenprodil are shown with quantification for $I_{ifen\text{-}sensitive}$ and τ for I_{NMDA}; $n = 6$–8 cells, 6–7 animals per genotype. (**b**,**c**) Hippocampal glutamate-receptor–subunit immunoblots (**b**, $n = 9$–12) and NR2B surface/total ratio (**c**, $n = 6$ slices, 3 animals per genotype) are shown. (**d**) Effects of ifenprodil (20 μM) and AP5 (50 μM) on LTP enhancement, with representative baseline (1,2) and 60-min (3,4) traces ($n = 6$). (**e**) Calpain-mediated NR2B cleavage in hippocampal slices after NMDA treatment. Cleaved NR2B (cNR2B) was detected with Tub loading control after 30- or 60-min treatment with buffer, 50 μM NMDA or 50 μM NMDA/20 μM calpeptin (Cal; $n = 4$–6). (**f**) Calpain-mediated degradation of NR2B *in vitro* in the presence or absence of Cdk5/p25 ($n = 3$). (**g**) Coimmunoprecipitation of NR2B, Cdk5 and calpain-1 from WT hippocampus. Lysates or immunoprecipitates derived using the antibodies indicated (IP) were immunoblotted for the proteins denoted (left). Representative of eight experiments. (**h**) Cytoplasmic NR2B, Cdk5 and calpain binding assays. Immobilized NR2B C terminus (top) or Cdk5/p25 (bottom) were incubated with Cdk5/p25, NR2B and/or unactivated calpain. Immunoblots show selective binding of Cdk5, NR2B and calpain. Representative of 12 experiments. Data represent mean ± s.e.m.; $^*P < 0.05$, $^{**}P < 0.01$, $^{***}P < 0.05$ *post hoc* versus WT; Student's *t*-test.

of memory, it will be necessary to clarify the relationship between plasticity and learning suggested here. Furthermore, although we have focused on the role of Cdk5 in regulating functional plasticity via NMDARs, Cdk5 knockout likely affects learning via additional pathways. Nonetheless, these observations reveal a previously unknown molecular mechanism through which Cdk5 directly interacts with the NR2B NMDAR subunit and calpain to facilitate NR2B degradation. Through such interactions, Cdk5 may influence NMDAR constituency, synaptic plasticity and learning.

METHODS

Knockout generation, histology and molecular biology. The floxed line was generated as previously described[37]. We crossed floxed Cdk5 and Cre-ERT mice[14] and treated F3 male offspring with 4-hydroxytamoxifen (15 d, 66.67 mg per kg of body weight, intraperitoneal). All experiments were carried out with 10–12-week-old males, 2–4 weeks after treatment. PCR genotyping with primers encompassing *loxP* sites or within the Cre-ER^T transgene were used to distinguish genotypes. Primers for Cdk5 allele genotyping had the following nucleotide sequences: 5′-GCAGGCCTTCGTTCCTCCC-3′ and 5′-CCTGA CACGCTTCAGAGCC-3′. Primers for the Cre-ER^T transgene had the following sequences: 5′-CAACCGAGCTGAAGCATTCTGCC-3′ and 5′-CATCAAC GTTTTCTTTTCGGATC-3′. The template for the Cdk5 *in situ* hybridization probe was created from mouse brain cDNA using the primers 5′-GCGCG GTACCACCTACGGAACTGTGTT-3′ and 5′-GTCGCCGCGGCTTCACAATC TCAGGG-3′. Radiolabeled *in situ* hybridizations were carried out as described[38,39]. Quantitative RT-PCR was performed as described[39] on whole hippocampus using the Cdk5 primers 5′-GGCTAAAAACCGGGAAACTC-3′ and 5′-CCATTGCAGCTGTCGAAATA-3′, the NR2B primers 5′-TCTGCCTT CTTAGAGCCATT CAG-3′ and 5′-AGACAGCTACAGCAGAGAC-3′, the NR2A primers 5′-CCTCGAACC CTTCAGCGCCT-3′ and 5′-AATGGCAGAGACAAT GAGCAG-3′ and the NR1 primers 5′-GCAGGTGGAGTTGAGCACCATGTA C-3′ and 5′-AGCTTGTTGTCCCGCACA-3′. Cdk5 from glia and presynaptic terminals from nonhippocampal regions may have contributed to the Cdk5 signal measured using RT-PCR, immunoblot and activity analyses. For more accurate and higher-resolution analysis, FISH was carried out using digoxigenin-labeled mRNA probes and analyzed with confocal microscopy, essentially as decribed[39].

Biochemistry. Immunoblots, immunoprecipitations, immunoprecipitation-kinase assays, *in vitro* phosphorylation reactions and surface-labeling experiments were carried out using standard methodologies[4,6,29,38]. All immunoblot quantification is shown relative to tubulin loading controls.

Synaptosomal preparations were prepared as follows: hippocampi or cortex and striatum from three knockout or wild-type mice were dissected and homogenized with buffer A containing 5 mM Tris-HCl (pH 7.4), 1 mM $MgCl_2$, 0.5 mM $CaCl_2$, 1 mM NaF, 0.1 mM PMSF and protease cocktail inhibitor. The homogenized sample was centrifuged at 1,400*g* for 10 min to obtain the P1 and S1 fractions. The P1 fraction was resuspended with buffer A and centrifuged at 700*g* for 10 min to obtain the S1′ fraction. The S1 and S1′ fractions were mixed and centrifuged at 13,800*g* for 10 min to obtain the P2 fraction (pellet). The P2 fraction was resuspended in buffer B containing 6 mM Tris-HCl (pH 8.0), 1 mM NaF, 0.1 mM PMSF and 0.32 mM sucrose containing protease cocktail inhibitor, and layered on the top of a discontinuous sucrose gradient consisting of 0.85 M, 1.0 M and 1.25 M sucrose. The gradient was centrifuged at 82,500*g* for 2 h. The synaptosome fraction was collected and centrifuged at 38,200*g* for 20 min. The pellet was lysed with lysis buffer

containing 1% SDS and 50 mM NaF, and subjected to SDS-PAGE and immunoblot analysis.

To examine NR2B biochemically, we purified the recombinant full-length C terminus of NR2B-GST (plasmid kindly provided by K.U. Bayer, University of Colorado Health Sciences Center), GST and protein phosphatase inhibitor–1 using standard protein purification techniques. Cdk5 purification and *in vitro* kinase reactions were carried out as described[4]. For coimmunoprecipitations, hippocampal lysates in RIPA buffer were incubated with primary antibodies, and then with protein-A–conjugated resin at 4 °C before washes and SDS-PAGE and immunoblot analysis. For binding assays, purified NR2B-GST or GST was rebound to glutathione-Sepharose resin. Cdk5 was reconjugated to Ni^{2+} agarose. Protein/resin and controls were washed, incubated in Ca^{2+}-free buffer with potential binding partners (NR2B, Cdk5 and/or calpain-1) for 1 h at 4 °C, washed again, and then analyzed by immunoblotting. *In vitro* calpain-mediated NR2B degradation assays were carried out similarly as described[24]. Recombinant full-length C terminus of NR2B (0.5 μM) was incubated at 4 °C for 90 min in the presence of inactive Cdk5/p25 to allow for binding. The time course of NR2B degradation was conducted at 37 °C after the addition of Ca^{2+}-activated calpain-1 (Sigma, 1:1,000). Cdk5 and calpain activities were blocked with ATP-free and Ca^{2+}-free conditions, respectively.

Hippocampal slices were prepared as follows: 400-μm transverse hippocampal slices were prepared in ice-cold Krebs buffer and then allowed to recover in oxygenated Krebs buffer (30 °C) for 30 min, similarly as described[40]. Slices were then incubated in 50 μM NMDA for 30 or 60 min or in Krebs buffer for 60 min. Additional slices were incubated for 60 min in 50 μM NMDA and 20 μM calpeptin to confirm calpain dependence of cNR2B generation.

Behavior. Mice were housed four or five per cage in a colony maintained at 23 °C with a 12-h light/dark cycle (lights on from 7:00 a.m. to 7:00 p.m.) and *ad libitum* food and water. All procedures were approved by the University of Texas Southwestern Institutional Animal Care and Use Committee. Behavior was carried out with the experimenter blind to genotype. Contextual and cue fear conditioning were performed using one or two 1-s, 0.8-mA foot shocks, respectively, as described[41]. For extinction trials, freezing to the conditioned context was assessed for 5 min, 24 h, 48 h, 72 h and 96 h after training and normalized to the 24-h-post-training value. Nociceptive responses were determined by measuring the stimulus threshold to elicit flinching, jumping and vocalizing as described[41]. Hotplate latency to hind-paw lick, jumping or vocalization was assessed after animals were placed on a 52 °C hotplate. Locomotor activity and elevated plus anxiety maze was carried out, similarly as described[41]. For the open-field anxiety test, each animal was placed in the center of a Plexiglas box under standard room-lighting conditions. Locomotor activity was quantified using the number of photoreceptor beam breaks and open-field anxiety was measured as the time spent in the center of the box using a standard computer tracking system. The water-maze task was carried out essentially as described[41].

Neurophysiology. Transverse hippocampal slices were prepared in cutting saline (200 mM sucrose, 3 mM KCl, 1.4 mM NaH_2PO_4, 26 mM $NaHCO_3$, 2 mM $MgCl_2$, 2 mM $CaCl_2$ and 10 mM glucose) and maintained in an interface chamber containing artificial cerebrospinal fluid[42]. Extracellular SC-CA1 voltage measurements in field recordings (fEPSPs) were synaptically evoked at 0.033 Hz and performed at 27 °C. Weak TBS (2×) and strong TBS (3×) were defined as 10 and 15 bursts, respectively (four pulses per burst at 100 Hz, 5-Hz burst frequency). Tetani were delivered at 50 and 100 Hz for 1 s. Basal input/output measurements, PPF and LTP experiments were carried out in the absence of any drugs, whereas $fEPSP_{NMDA}$ and fEPSP NMDA/AMPA measurements were performed in the presence of 2 μM SR95531, 1 μM atropine, 50 μM $NiCl_2$, 10 μM nimodipine and 50 nM tetrodotoxin. NMDAR-mediated fEPSPs were recorded in the presence of 20 μM 6,7-dinitroquinoxaline-2,3-dione (DNQX) and blocked with 50 μM AP5. fEPSP data acquisition and analysis were carried out using the multielectrode MED64 hardware and software packages, essentially as described[43]. Additional analyses were performed using custom macros running in Igor Pro and Microsoft Excel. Whole-cell voltage-clamp SC-CA1 EPSCs were recorded, using instruments similar to those described[42], to more selectively isolate NMDAR-mediated currents and eliminate threshold nonlinearities. Whole-cell recording electrodes (2–3 MΩ) were filled with a 7.3 pH intracellular cell solution containing 110 mM D-gluconic acid, 110 mM CsOH, 20 mM CsCl, 10 mM disodium phosphocreatine, 0.3 mM sodium GTP, 2 mM magnesium ATP, 10 mM HEPES, 0.5 mM EGTA and 5 mM lidocaine *N*-ethyl bromide. EPSCs were evoked at 0.05 Hz at 32 °C, and stimulus intensity was chosen to elicit 125–150-pA EPSCs at –70-mV holding potential. Before each sweep, a –5-mV step pulse was injected to assess and control for series resistance. τ for EPSCs was calculated with a single-exponential fit. Whole-cell recordings were carried out in the presence of 2 μM SR95531, 1 μM atropine, 50 μM $NiCl_2$ and 10 μM nimodipine. NMDAR-mediated EPSCs were isolated at +40 or +60 mV in the presence of 20 μM DNQX and blocked with 50 μM AP5. NMDA/AMPA EPSC ratio was calculated under +40 mV/20 μM DNQX and –70 mV conditions. An alternative whole-cell SC-CA1 EPSC NMDA/AMPA ratio was calculated in the absence of DNQX: the NMDA component was measured as the area of the +40 mV EPSC from 45 ms to 350 ms in 2 μM SR95531, 1 μM atropine, 50 μM $NiCl_2$ and 10 μM nimodipine. Ifenprodil-sensitive NMDAR-mediated currents were recorded at a +60 mV holding potential in the presence of 20 μM DNQX. Quantification for $I_{ifen\text{-}sensitive}$ was calculated as the area between I_{NMDA} and $I_{ifen\text{-}resistant}$, normalized to I_{NMDA}. Whole-cell data acquisition and analysis were carried out using custom macros running in Igor Pro, Microsoft Excel and GraphPad Prism.

Note: Supplementary information is available on the Nature Neuroscience website.

ACKNOWLEDGMENTS

We thank B. Potts, S. Gold, J. Pick and M. Waung for assistance with experiments, D. Metzger for characterization of Cre-ER^T line, C. Steffen for assistance with animal husbandry and K. Bayer for the NR2B clone. We thank A. Nairn and E. Nestler for comments and discussion and are grateful to the Medical Scientist Training Program at the University of Texas Southwestern Medical Center. This work was made possible by the US National Institutes on Drug Abuse National Research Service Award training grant (A.H.H.), US National Institutes of Health individual National Research Service Awards (D.R.B., C.N.), US National Alliance for Research on Schizophrenia and Depression Young Investigator awards (C.M.P. and D.C.C.), grant funding from the US National Institutes on Drug Abuse (P.G., D.C.C. and J.A.B.) and Mental Health (P.G., C.M.P. and J.A.B.) and the Ella McFadden Charitable Trust Fund at the Southwestern Medical Foundation (J.A.B).

AUTHOR CONTRIBUTIONS

A.H.H. performed knockout optimization, histology, learning behavior testing, extracellular recordings, slice pharmacology, biochemistry and data analysis. D.R.B. established the mouse colony, optimized genotyping and histology and performed anxiety behavior testing. C.N. performed whole-cell voltage-clamp recordings. J.W.K. assisted in genotyping and histology. K.H. prepared synaptosomes and recombinant Cdk5. P.C. and P.G. provided mouse lines. C.M.P., D.C.C. and J.A.B. designed and supervised the experiments conducted in their laboratories. A.H.H. and J.A.B. prepared the manuscript. All authors contributed to experimental design, discussed the results and commented on the report.

COMPETING INTERESTS STATEMENT

The authors declare no competing financial interests.

Published online at http://www.nature.com/natureneuroscience
Reprints and permissions information is available online at http://npg.nature.com/reprintsandpermissions

1. Sweatt, J.D. *Mechanisms of Memory* (Elsevier, San Diego, California, 2003).
2. Whitlock, J.R., Heynen, A.J., Shuler, M.G. & Bear, M.F. Learning induces long-term potentiation in the hippocampus. *Science* **313**, 1093–1097 (2006).
3. Bibb, J.A. *et al.* Effects of chronic exposure to cocaine are regulated by the neuronal protein Cdk5. *Nature* **410**, 376–380 (2001).
4. Bibb, J.A. *et al.* Phosphorylation of DARPP-32 by Cdk5 modulates dopamine signalling in neurons. *Nature* **402**, 669–671 (1999).
5. Cheung, Z.H., Fu, A.K.Y. & Ip, N.Y. Synaptic roles of Cdk5: implications in higher cognitive functions and neurodegenerative diseases. *Neuron* **50**, 13–18 (2006).
6. Fischer, A., Sananbenesi, F., Pang, P.T., Lu, B. & Tsai, L.H. Opposing roles of transient and prolonged expression of p25 in synaptic plasticity and hippocampus-dependent memory. *Neuron* **48**, 825–838 (2005).
7. Fischer, A., Sananbenesi, F., Schrick, C., Spiess, J. & Radulovic, J. Cyclin-dependent kinase 5 is required for associative learning. *J. Neurosci.* **22**, 3700–3707 (2002).

8. Gilmore, E.C., Ohshima, T., Goffinet, A.M., Kulkarni, A.B. & Herrup, K. Cyclin-dependent kinase 5–deficient mice demonstrate novel developmental arrest in cerebral cortex. *J. Neurosci.* **18**, 6370–6377 (1998).
9. Ohshima, T. *et al.* Impairment of hippocampal long-term depression and defective spatial learning and memory in p35 mice. *J. Neurochem.* **94**, 917–925 (2005).
10. Ohshima, T. *et al.* Targeted disruption of the cyclin-dependent kinase 5 gene results in abnormal corticogenesis, neuronal pathology and perinatal death. *Proc. Natl. Acad. Sci. USA* **93**, 11173–11178 (1996).
11. Patrick, G.N. *et al.* Conversion of p35 to p25 deregulates Cdk5 activity and promotes neurodegeneration. *Nature* **402**, 615–622 (1999).
12. Wei, F.Y. *et al.* Control of cyclin-dependent kinase 5 (Cdk5) activity by glutamatergic regulation of p35 stability. *J. Neurochem.* **93**, 502–512 (2005).
13. Yan, Z., Chi, P., Bibb, J.A., Ryan, T.A. & Greengard, P. Roscovitine: a novel regulator of P/Q-type calcium channels and transmitter release in central neurons. *J. Physiol. (Lond.)* **540**, 761–770 (2002).
14. Weber, P., Metzger, D. & Chambon, P. Temporally controlled targeted somatic mutagenesis in the mouse brain. *Eur. J. Neurosci.* **14**, 1777–1783 (2001).
15. Tang, Y.P. *et al.* Genetic enhancement of learning and memory in mice. *Nature* **401**, 63–69 (1999).
16. Tsien, J.Z., Huerta, P.T. & Tonegawa, S. The essential role of hippocampal CA1 NMDA receptor–dependent synaptic plasticity in spatial memory. *Cell* **87**, 1327–1338 (1996).
17. Bernasconi-Guastalla, S., Wolfer, D.P. & Lipp, H.P. Hippocampal mossy fibers and swimming navigation in mice: correlations with size and left-right asymmetries. *Hippocampus* **4**, 53–63 (1994).
18. Nakazawa, K. *et al.* Hippocampal CA3 NMDA receptors are crucial for memory acquisition of one-time experience. *Neuron* **38**, 305–315 (2003).
19. Angelo, M., Plattner, F., Irvine, E.E. & Giese, K.P. Improved reversal learning and altered fear conditioning in transgenic mice with regionally restricted p25 expression. *Eur. J. Neurosci.* **18**, 423–431 (2003).
20. Monyer, H., Burnashev, N., Laurie, D.J., Sakmann, B. & Seeburg, P.H. Developmental and regional expression in the rat brain and functional properties of four NMDA receptors. *Neuron* **12**, 529–540 (1994).
21. Chenard, B.L. & Menniti, F.S. Antagonists selective for NMDA receptors containing the NR2B subunit. *Curr. Pharm. Des.* **5**, 381–404 (1999).
22. Picconi, B. *et al.* NR2B subunit exerts a critical role in postischemic synaptic plasticity. *Stroke* **37**, 1895–1901 (2006).
23. Liu, L. *et al.* Role of NMDA receptor subtypes in governing the direction of hippocampal synaptic plasticity. *Science* **304**, 1021–1024 (2004).
24. Guttmann, R.P. *et al.* Specific proteolysis of the NR2 subunit at multiple sites by calpain. *J. Neurochem.* **78**, 1083–1093 (2001).
25. Guttmann, R.P. *et al.* Proteolysis of the *N*-methyl-D-aspartate receptor by calpain *in situ*. *J. Pharmacol. Exp. Ther.* **302**, 1023–1030 (2002).
26. Simpkins, K.L. *et al.* Selective activation induced cleavage of the NR2B subunit by calpain. *J. Neurosci.* **23**, 11322–11331 (2003).
27. Zhao, M.G. *et al.* Roles of NMDA NR2B subtype receptor in prefrontal long-term potentiation and contextual fear memory. *Neuron* **47**, 859–872 (2005).
28. Kutsuwada, T. *et al.* Impairment of suckling response, trigeminal neuronal pattern formation and hippocampal LTD in NMDA receptor epsilon 2 subunit mutant mice. *Neuron* **16**, 333–344 (1996).
29. Chung, H.J., Huang, Y.H., Lau, L.F. & Huganir, R.L. Regulation of the NMDA receptor complex and trafficking by activity-dependent phosphorylation of the NR2B subunit PDZ ligand. *J. Neurosci.* **24**, 10248–10259 (2004).
30. Husi, H., Ward, M.A., Choudhary, J.S., Blackstock, W.P. & Grant, S.G. Proteomic analysis of NMDA receptor–adhesion protein signaling complexes. *Nat. Neurosci.* **3**, 661–669 (2000).
31. Lee, M.S. *et al.* Neurotoxicity induces cleavage of p35 to p25 by calpain. *Nature* **405**, 360–364 (2000).
32. Liu, M.C. *et al.* Comparing calpain- and caspase-3–mediated degradation patterns in traumatic brain injury by differential proteome analysis. *Biochem. J.* **394**, 715–725 (2006).
33. Dong, Y.N., Waxman, E.A. & Lynch, D.R. Interactions of postsynaptic density-95 and the NMDA receptor 2 subunit control calpain-mediated cleavage of the NMDA receptor. *J. Neurosci.* **24**, 11035–11045 (2004).
34. Morabito, M.A., Sheng, M. & Tsai, L.H. Cyclin-dependent kinase 5 phosphorylates the N-terminal domain of the postsynaptic density protein PSD-95 in neurons. *J. Neurosci.* **24**, 865–876 (2004).
35. Costa-Mattioli, M. *et al.* Translational control of hippocampal synaptic plasticity and memory by the eIF2alpha kinase GCN2. *Nature* **436**, 1166–1173 (2005).
36. Kiyama, Y. *et al.* Increased thresholds for long-term potentiation and contextual learning in mice lacking the NMDA-type glutamate receptor epsilon1 subunit. *J. Neurosci.* **18**, 6704–6712 (1998).
37. Wattler, S., Kelly, M. & Nehls, M. Construction of gene targeting vectors from lambda KOS genomic libraries. *Biotechniques* **26** 1150–6, 1158, 1160 (1999).
38. Gold, S.J., Ni, Y.G., Dohlman, H.G. & Nestler, E.J. Regulators of G-protein signaling (RGS) proteins: region-specific expression of nine subtypes in rat brain. *J. Neurosci.* **17**, 8024–8037 (1997).
39. Berton, O. *et al.* Essential role of BDNF in the mesolimbic dopamine pathway in social defeat stress. *Science* **311**, 864–868 (2006).
40. Nishi, A. *et al.* Regulation of DARPP-32 dephosphorylation at PKA- and Cdk5-sites by NMDA and AMPA receptors: distinct roles of calcineurin and protein phosphatase-2A. *J. Neurochem.* **81**, 832–841 (2002).
41. Powell, C.M. *et al.* The presynaptic active zone protein RIM1alpha is critical for normal learning and memory. *Neuron* **42**, 143–153 (2004).
42. Cooper, D.C., Chung, S. & Spruston, N. Output-mode transitions are controlled by prolonged inactivation of sodium channels in pyramidal neurons of subiculum. *PLoS Biol.* **3**, e175 (2005).
43. Itoh, K., Shimono, K. & Lemmon, V. Dephosphorylation and internalization of cell adhesion molecule L1 induced by theta burst stimulation in rat hippocampus. *Mol. Cell. Neurosci.* **29**, 245–249 (2005).